Conjugated Polymers

DOI: 10.1002/anie.201205653

Controllable Processes for Generating Large Single Crystals of Poly(3-hexylthiophene)**

*Khosrow Rahimi, Ioan Botiz, Natalie Stingelin, Navaphun Kayunkid, Michael Sommer, Felix Peter Vinzenz Koch, Ha Nguyen, Olivier Coulembier, Philippe Dubois, Martin Brinkmann, and Günter Reiter**

Extensive efforts have been taken to correlate the performance of organic optoelectronic devices with changes in molecular conformation, differences in long-range order,[1–3] and the various morphologies formed by conjugated polymers, for example, the regioregular poly(3-alkylthiophene)s (P3AT).[4–7] Gaining a full understanding of structure/processing/performance relationships requires optimal control of all structural parameters.[8] However, even in the simple geometry of thin films, where crystalline domains can be preferentially oriented, long-range in-plane order is difficult to achieve.[9] Interfacial regions and grain boundaries are often unavoidable and usually affect the electronic attributes, for example, charge transport, in an adverse way.[10,11] In this context, large single crystals characterized by a unique order of all the molecules across all length scales may provide suitable model systems that allow the determination of how the optoelectronic properties in semiconducting polymers depend on structural features ranging from the molecular to the macroscopic level.

However, the formation of large single crystals of conjugated polymers—indeed of all macromolecular species—is inherently difficult and often quite time consuming.[12] To date, reports on the growth of single crystals of conjugated polymers are scarce[12] and experimentally challenging.[13] As the nucleation probability of polymers is low and thus high under-cooling or over-saturation would be needed, we have employed a self-seeding approach to master the number density, size, shape, and orientation of the obtained large single crystals of regioregular poly(3-hexylthiophene) (P3HT), a semicrystalline conjugated polymer.

Self-seeding has been successfully used for the growth of single crystals of classical semicrystalline polymers.[14–17] As a consequence of the statistical process of chain folding, all polymer crystals—and thus also P3HT crystals—consist of regions with different degrees of order (chain folding, that is, variations in the thickness of the lamellae), which results in a broad range of melting or dissolution temperatures[14–17] (T_{DISS}; see Figure S1 in the Supporting Information). Prior to isothermal crystallization, solutions already containing crystalline aggregates were heated to the so-called seeding temperature (T_{SS}), which is below the maximum dissolution temperature ($T_{DISS,max}$) at which all molecules are homogeneously dissolved. At T_{SS}, only entities with a higher degree of order or a lower surface to volume ratio are stable and thus act as seeds for immediate crystallization at a lower temperature (T_C).[9,14–17] The seed density did not depend on the time t_{SS} the sample was kept at the T_{SS} value (see Figure S2 in the Supporting Information), thus indicating that the seeds were thermodynamically stable and not kinetically controlled.[14] To avoid heterogeneous or homogeneous nucleation on the timescale of the experiment, an appropriately high T_C value was chosen. Both the T_{SS} and T_C values were adjusted for the materials with different chain lengths, solution concentration, and the solvent. Thus, self-seeding allows independent control

[*] K. Rahimi, Dr. I. Botiz, Prof. G. Reiter
Institute of Physics, University of Freiburg
Hermann-Herderstrasse 3, 79104 Freiburg (Germany)
E-mail: guenter.reiter@physik.uni-freiburg.de
Dr. I. Botiz, Dr. N. Stingelin, Prof. G. Reiter
Freiburg Institute for Advanced Studies
Albertstrasse 19, 79104 Freiburg (Germany)
Dr. N. Stingelin
Department of Materials and Centre for Plastic Electronics
Imperial College London
Exhibition Road, London, SW7 2AZ (UK)
N. Kayunkid, Prof. M. Brinkmann
Institut Charles Sadron, CNRS Université de Strasbourg
23 rue du Loess, 67034 Strasbourg (France)
Dr. M. Sommer
Institute of Macromolecular Chemistry
University of Freiburg
Stefan-Meier-Strasse 31, 79104 Freiburg (Germany)
Dr. N. Stingelin, F. Koch
Institut für Polymere, Department of Materials
Eidgenössische Technische Hochschule (ETH) Zürich
Wolfgang-Pauli-Strasse 10, 8093 Zürich (Switzerland)
H. Nguyen, Dr. O. Coulembier, Prof. P. Dubois
Center of Innovation and Research in Materials and Polymers (CIRMAP), Laboratory of Polymeric and Composite Materials (LPCM), University of Mons
Place du Parc 23, 7000 Mons (Belgium)

[**] I.B., N.S., and G.R. acknowledge financial support from the Freiburg Institute for Advanced Studies (FRIAS). K.R. and G.R. acknowledge partial support by the German Research Foundation (DFG) as well as fruitful discussions with Barbara Heck, Roozbeh Shokri, and Kaiwan Jahanshahi. We are thankful to Noboru Osaka from Tokyo University of Agriculture and Technology, Tokyo (Japan) for some preliminary experiments. This work has also been partially supported by the European Commission and Région Wallonne FEDER program (Materia-Nova), the OPTI²MAT program of excellence by the Interuniversity Attraction Pole program of the Belgian Federal Science Policy office (PAI 6/27), and by the FNRS-FRFC. O.C. is a FNRS Research Associate.

Supporting information for this article is available on the WWW under http://dx.doi.org/10.1002/anie.201205653.

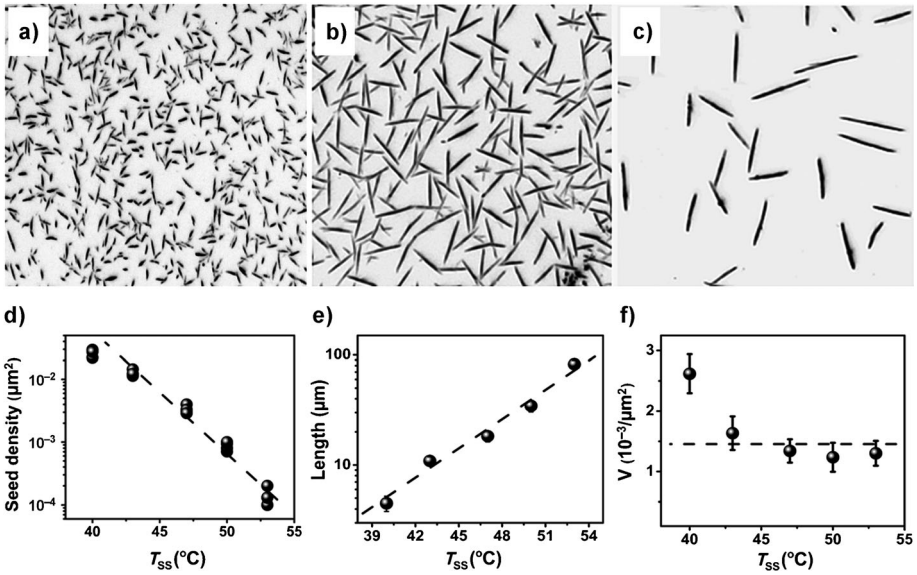

Figure 1. Optical micrographs of single crystals of P3HT-26, obtained from a 0.2 mg mL^{-1} solution of 3-hexylthiophene crystallized at 32 °C for 24 h and spin coated onto silicon substrates, for seeds formed at: a) 40 °C, b) 43 °C, and c) 47 °C. Note that all the crystals in each image are about the same size. All images represent an area of 100×100 μm^2. d) Corresponding density of seeds *N* that remain in the P3HT-26 solution as a function of the T_{SS} value, inferred from counting the crystal density. The value *N* did not vary with a seeding time of 6 and 12 h, respectively. e) Length of single crystals of P3HT-26 as a function of T_{SS}. f) Corresponding approximate volume of all crystals per unit area as a function of T_{SS}, obtained by multiplying *N* by the mean length and cross-section of the crystals.

over the seed density and growth rate by varying the T_{SS} and T_C values, respectively.

Figure 1 a–c show a series of optical micrographs of self-seeded single crystals of P3HT ($M_n = 26$ kg mol^{-1}; that is, P3HT-26) grown after initial seeding at various values of T_{SS}. The anisotropic shape of the crystal is due to faster growth along the direction involving strong π–π interactions between the thiophene rings, which represents the longest axis of the crystal (see below), and is consistent with the needlelike single crystals observed, for example, in phase-field simulations.[18] As expected, the number density of surviving seeds (nuclei) depended on the T_{SS} value:[9,16,17] fewer crystals, albeit of larger dimensions, were observed at higher values of T_{SS}. Counting the number density (*N*) of these crystals provided a direct way of determining the density of the self-seeding nuclei present at the T_{SS} (see Figure 1 d). Consistent with previous studies,[9,16,17] the value of *N* decreased significantly (approximately exponentially) with increasing T_{SS} values. Homogeneous nucleation was not observed on the timescale of the experiment. No crystals formed at the temperature T_C when the solution was heated to well above the $T_{DISS,max}$ value.

Figure 1 e shows that the average length (*L*) of the long axis of self-seeded single crystals of P3HT-26 increased markedly with the T_{SS} value. All crystals had approximately the same size at a given T_{SS} value. In a supersaturated solution containing seeds at T_C, all the crystals started to grow simultaneously and at the same rate, but only until the decreasing concentration of the solution surrounding the crystals had reached the solubility limit and crystal growth stopped. As the amount of molecules above the solubility limit was constant and independent of the number of growing crystals, a decrease in *N* with an increase in the T_{SS} value resulted in the maximum size of the resulting crystals changing reciprocally. Thus, millimeter-sized single crystals can be obtained at very low seeding densities, which is consistent with the results shown in Figure 1 d,e. As a control, Figure 1 f shows that for a given T_C value, the approximate volume (*V*) of all the deposited P3HT-26 single crystals per unit area was independent of T_{SS} (*V* is related to the amount of polymer above the solubility limit). The somewhat higher value of *V* at 40 °C is most likely due to a higher probability of polymers encountering a crystal and attaching to it, thus causing a depletion of the surrounding solution.

To prove that the objects seen in Figure 1 were indeed single crystals we used selected-area electron diffraction (SAED) and determined the characteristic spacings of the corresponding crystalline unit cell. Figure 2 a displays a representative SAED pattern of a P3HT-26 single crystal. This pattern is characteristic of a monoclinic crystal structure probed with the electron beam along the polymer chain direction, that is, along the normal of the substrate plane. By using defocused diffraction (Figure 2 b) we were able to determine the relative orientation of the unit cell with respect to the long axis of the P3HT crystals. As expected, the *b*-axis corresponds to the long axis of the P3HT single crystals, thus supporting that the direction of fast growth is determined by π stacking. A height profile of a typical P3HT-26 single crystal, as obtained by atomic force microscopy (AFM, Figure 2 c) indicates that the height of the crystals was quite uniform. P3HT can adopt different forms, with form I being most commonly observed in thin films, while form II represents an energetically more stable situation. Interestingly, from the SAED pattern we deduced repeat distances of (1.31 ± 0.05) nm and (0.924 ± 0.05) nm along the *a*-direction and the π-stacking direction (*b*-axis), respectively, thus indicating significant interdigitation of the hexyl chains and thus suggesting P3HT crystals of form II. The angle between the *a*- and *b*-axis was $\gamma = 68°$. A schematic depiction of the arrangements of the polymers in the crystals is given in Figure 2 d,e.

The values of the unit cell parameters *b* and γ obtained for P3HT are similar to those of form II of poly(3-butylthiophene) (P3BT),[19] which further supported the identification of the polymorph structure.[4,18] The π-stacking distance ($d_{\pi\text{-}\pi} = {}^1/_2 \times 0.924\ \text{nm} \times \sin\gamma$) of approximately 0.43 nm is also consistent with the predicted value of 0.44 nm for the energetically stable structure in form II.[20] By using a mono-

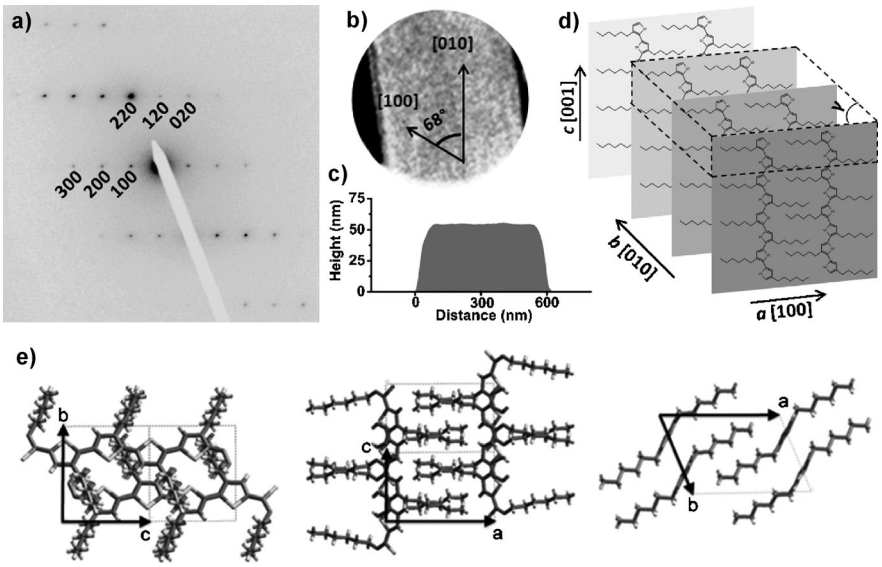

Figure 2. a) Selected-area electron diffraction (SAED) pattern of a P3HT-26 single crystal formed at 35 °C for 24 h after being previously seeded at 50 °C for 6 h. A repeat distance of 9.24 Å along the π-stacking direction "*b*", and a repeat distance of 13.08 Å along the alkyl side chain direction "*a*" were obtained. The SAED pattern was obtained for an incident beam parallel to the chain axis "*c*" of the P3HT-26 molecules in the single crystal. b) Defocused diffraction pattern in the proper relative orientation to the electron diffraction pattern. The directions of the direct space unit cell axes are also indicated. c) AFM height profile of a P3HT-26 single crystal (the height of a single crystal corresponds to the lamellae thickness). d) Schematic representation of the orientation of the P3HT-26 chains inside the single crystal. The size of the monoclinic unit cell is indicated by the broken lines. e) Projection of the refined crystal structure along the three crystallographic axes. Note the tip edge of the crystal corresponding to a (110) growth face. This plane contains the 3-hexyl side chains.

clinic unit cell with a $P2_{1/c}$ space group, similar to that proposed by Buono et al. for P3BT[19] ($a = 1.076$ nm, $b = 0.944$ nm, $c = 0.777$ nm (chain axis), and $\gamma = 64.66°$), we obtained, by trial and error, a structural model (Figure 2e) that leads to a very good agreement between the experimental and calculated SAED patterns for the [001] zone. In particular, the relative intensities of the intense {220} and the faint {120} reflections were reproduced very well. 2D projections of the results of this structural model (Figure 2e) show the strongly interdigitated *n*-hexyl side chains. As a consequence of the strong inclination of the plane of the polythiophene backbone with respect to the *b*-axis, the large 0.43 nm interchain distance between two chains along the *b*-axis results in 0.33 nm interchain contacts (Figure 2e, projection on the (*a*,*b*) plane), that is, a distance favorable for π stacking that is similar to the more common form I.[21] Interestingly, the (110) growth face containing the hexyl side chains is almost parallel to the plane of the polythiophene backbones, and the strong interaction of two successive planes through π stacking explains why this is the fast growth face.

The highly ordered internal structure of unique molecular orientation over the whole area of the P3HT-26 single crystals was confirmed by complementary birefringence measurements using optical microscopy with crossed polarizers (POM). Figure 3a,c shows highly birefringent P3HT-26 single crystals that were crystallized at temperatures differing by 3 °C. The birefringence of crystals grown at the higher T_C value of 35 °C was highly uniform across the entire crystal area (Figure 3c), while crystals grown at the lower T_C value of 32 °C were noticeably more inhomogeneous, thus indicating a lower degree of internal order in these samples. These observations are consistent with the SAED patterns (Figure 3b,d), when taking into account the differences in sensitivity between the two approaches.

To verify if the observed lattice parameters represent general features of P3HT crystals, we have compared the results for P3HT-26 with single crystals grown from P3HT samples with other molecular weights, synthesized by different methods and with different degrees of regioregularities (see Table 1 and the Supporting Information). As observed in the unit cell parameters of P3HT crystals of form I, one may also expect an increase in the long axis *a* as the molecular weight increases.[20] Figure 4a–c shows the optical micrographs and Figure 4d–f shows the corresponding SAED patterns of crystals of TH_8, P3HT-4,[22] and P3HT-5,[23] respectively. The uniform brightness of the birefringent crystals detected by POM is consistent with

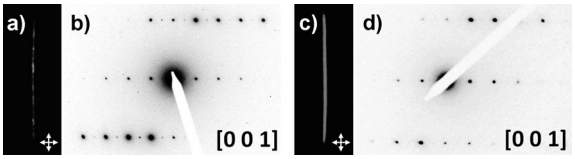

Figure 3. Optical micrographs (18×45 μm²) under crossed polarizers and corresponding selected area electron diffraction patterns of P3HT-26 crystals grown, after initial seeding at 50 °C, at a,b) 32 °C for 24 h and c,d) 35 °C for 36 h, respectively.

sharp reflexes in the SAED patterns, thus representing (similar to P3HT-26) well-ordered crystals consisting of molecules oriented with their main axis perpendicular to the substrate and with the direction of π stacking being along the long axis of the crystals (see summary in Table 1). Similar to P3HT-26, all these crystals corresponded to form II, but the unit cell parameter *a* increased monotonically with molecular weight. All the crystals grew at a similar rate, but longer molecules may have had an increased difficulty to perfectly incorporate into a crystal. In analogy to results for polyethyl ether ketone (PEEK),[24] the increase in the value of the *a*-axis parameter was attributed to the increase in the stress exerted by longer reentrant chains of longer polymers.

In contrast to the other samples, which all exhibited a characteristic asymmetry of the {*hk0*} reflections—a fingerprint of form II crystals—the SAED pattern of the short oligomer TH_8 (see Figure 4d) showed symmetric intensities

Table 1: Summary of crystallization conditions and structural parameters for the P3HT single crystals obtained in this work.

Sample	TH_8	P3HT-4	P3HT-5	P3HT-26
M_n [g mol^{-1}][a]	1332	3709	4700	26 400[b]
PDI	1.00	1.13	1.10	1.79
contour length (l_c)	3 nm	8.2 nm	10.6 nm	59 nm[c]
RR [%]	100	100	98.5	96.2
solvent	THF	3-HT	3-HT	3-HT
C_P [mg mL^{-1}]	10	2	2	0.2
T_{DISS} [°C]	ca. 25	ca. 40	ca. 38	ca. 55
T_C [°C]	2	10	10	35
t_C [h]	8	12	12	24
G.R. [μm^3 h^{-1}][d,e]	8.10 ± 2.11	0.42 ± 0.11	0.35 ± 0.10	0.30 ± 0.03
a (nm) ±0.05 nm	1.32	1.26	1.23	1.31
b (nm) ±0.05 nm	0.95	0.92	0.91	0.93
γ [°] ±0.5°	69.1	68.3	68.3	68.5

[a] Number average molecular weight (M_n) from MALDI-TOF, except for P3HT-26. [b] M_n from GPC. [c] l_c for P3HT-26 was obtained from the peak molecular weight (M_p = 50 300 g mol^{-1}). [d] For the low-molecular-weight samples crystallization was initiated through homogeneous nucleation. Consequently, the resulting crystals varied greatly in size. Only the largest crystals (nucleated at an early stage) were considered for the estimation of the growth rate. [e] Growth rate (G.R.) = LWH/$t_{C,max}$, where L, W, and H are respectively length, width, and height of the single crystal measured by AFM at maximum crystallization time $t_{C,max}$. PDI = polydispersity index, RR = regioregularity.

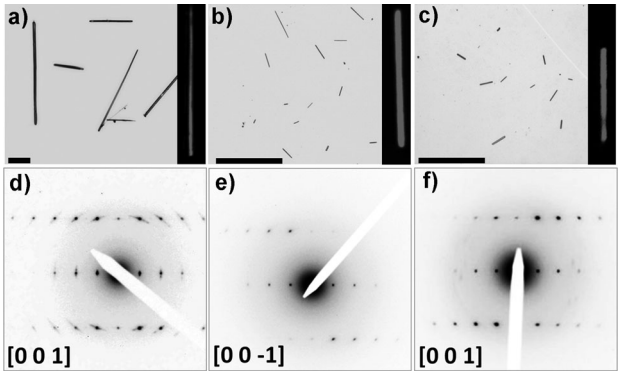

Figure 4. Optical micrographs of a) TH_8 single crystals grown in THF at 2 °C for 8 h; b) P3HT-4 crystals grown in 3-HT at 10 °C for 12 h; c) P3HT-5 crystals grown in 3-HT at 10 °C for 12 h. The scale bar represents 30 μm. The variable size of the crystals indicates that crystals did not start to grow simultaneously, thereby suggesting homogeneous nucleation. SAED patterns from a d) TH_8 single crystal; e) P3HT-4 single crystal; f) P3HT-5 single crystal. The uniform brightness across the whole crystal (a–c) and the sharp reflexes in the SAED patterns indicate the formation of well-ordered crystals containing unique oriented polymer chains.

of the reflections with respect to the meridian. The SAED pattern of TH_8 can be attributed to the superposition of patterns corresponding to the [001] and [00−1] zones, which result either from twinning of the crystal along the (*b*,*c*) plane or from stacking of crystalline lamellae. Twining is, however, less probable as one would expect twining also to occur for the longer polymeric chains, which is in contrast to our observations. Thus, it is more likely that the TH_8 crystals consist of stacks of lamellae crystals, which share a common orientation of the (*b*,*c*) plane but have either a [001] or [00−1] orientation; this is consistent with the observed thickness of up to several hundreds of nanometers (see Figure S3 in the Supporting Information). Interestingly, although P3HT-4[22] and P3HT-5 also formed stacks of lamellae, their SAED patterns showed asymmetry of the {*hk0*} reflections. On the basis of the SAED patterns, all the crystalline objects in the stacked lamellae can be considered as single crystals, as all the lamellae were arranged with perfect registry to each other.

We note that the slightly different processing conditions (e.g. faster growth rate) for TH_8 compared to the longer P3HT chains may have contributed to the less-dense packing of TH_8. Moreover, as the nucleation and growth of TH_8 in 3-HT would have to be performed at experimentally inaccessibly low temperatures, a change to tetrahydrofuran (THF) as a solvent of lower solubility was required. It has been suggested[25] that a higher solubility leads to a more pronounced interdigitation of the side chains. As can be seen in Table 1, the use of a slightly poorer solvent such as THF during crystallization yielded a lower degree of side-chain interdigitation and a lager distance in the π-stacking direction.

In summary, we have demonstrated that large single crystals can be grown not only from short regioregular oligomers but even from long poly(3-hexylthiophene) chains by employing a self-seeding approach and precisely controlling T_{SS}, T_C, and t_C values. The procedure allows control over the number density, size, and internal structure of these crystals. Materials obtained by different synthetic protocols with different degrees of regioregularity and different molecular weights all form single crystals of the monoclinic form II with interdigitated hexyl side groups when appropriately crystallized. It may be expected that the differences in lattice parameters and long-range order, although being typically quite small, will have a measurable impact on optoelectronic properties. Thus, such large single crystals comprised of semiconducting chains of the same molecular conformation over many length scales will represent valuable model systems to be used in molecular devices. This will finally enable the investigation of fundamental structure–optoelectronic property relationships, including anisotropy of, for example, charge transport as a function of molecular orientation within the crystal.

Received: July 16, 2012
Published online: September 28, 2012

Keywords: conjugation · crystal growth · poly(3-hexylthiophene) · polymers · single crystals

[1] H. Sirringhaus, P. J. Brown, R. H. Friend, M. M. Nielsen, K. Bechgaard, B. M. W. Langeveld-Voss, A. J. H. Spiering, R. A. J. Janssen, E. W. Meijer, P. Herwig, D. M. de Leeuw, *Nature* **1999**, *401*, 685 – 688.
[2] A. Salleo, R. J. Kline, D. M. DeLongchamp, M. L. Chabinyc, *Adv. Mater.* **2010**, *22*, 3812 – 3838.
[3] F. C. Grozema, L. D. A. Siebbeles, *J. Phys. Chem. Lett.* **2011**, *2*, 2951 – 2958.
[4] T. J. Prosa, M. J. Winokur, R. D. McCullough, *Macromolecules* **1996**, *29*, 3654 – 3656.

[5] K. J. Ihn, J. Moulton, P. Smith, *J. Polym. Sci. Part B* **1993**, *31*, 735 – 742.
[6] J. Liu, R. Zhang, G. Sauvé, T. Kowalewski, R. D. McCullough, *J. Am. Chem. Soc.* **2008**, *130*, 13167 – 13176.
[7] Y. Kim, S. Cook, S. M. Tuladhar, S. A. Choulis, J. Nelson, J. R. Durrant, D. D. C. Bradley, M. Giles, I. McCulloch, C. Ha, M. Ree, *Nat. Mater.* **2006**, *5*, 197 – 203.
[8] A. Salleo, *Mater. Today* **2007**, *10*, 38 – 45.
[9] E. J. W. Crossland, K. Rahimi, G. Reiter, U. Steiner, S. Ludwigs, *Adv. Funct. Mater.* **2011**, *21*, 518 – 524.
[10] M. J. Lee, D. Gupta, N. Zhao, M. Heeney, I. McCulloch, H. Sirringhaus, *Adv. Funct. Mater.* **2011**, *21*, 932 – 940.
[11] E. J. W. Crossland, K. Tremel, F. Fischer, K. Rahimi, G. Reiter, U. Steiner, S. Ludwigs, *Adv. Mater.* **2012**, *24*, 839 – 844.
[12] J. Lim, F. Liu, S. Ferdous, M. Muthukumar, A. L. Briseno, *Mater. Today* **2010**, *13*, 14 – 24.
[13] A. A. Virkar, S. Mannsfeld, Z. Bao, N. Stingelin, *Adv. Mater.* **2010**, *22*, 3857 – 3875.
[14] D. J. Blundell, A. Keller, A. J. Kovacs, *J. Polym. Sci. B* **1966**, *4*, 481 – 486.
[15] M. Tian, M. Dosiere, S. Hocquet, P. J. Lemstra, J. Loos, *Macromolecules* **2004**, *37*, 1333 – 1341.
[16] J. Xu, Y. Ma, W. Hu, M. Rehahn, G. Reiter, *Nat. Mater.* **2009**, *8*, 348 – 353.
[17] J. Qian, G. Guerin, Y. Lu, G. Cambridge, I. Manners, M. A. Winnik, *Angew. Chem.* **2011**, *123*, 1660 – 1663; *Angew. Chem. Int. Ed.* **2011**, *50*, 1622 – 1625.
[18] L. Gránásy, T. Pusztai, T. Börzsönyi, J. A. Warren, J. F. Douglas, *Nat. Mater.* **2004**, *3*, 645 – 650.
[19] A. Buono, N. H. Son, G. Raos, L. Gila, A. Cominetti, M. Catellani, S. V. Meille, *Macromolecules* **2010**, *43*, 6772 – 6781.
[20] M. Brinkmann, *J. Polym. Sci. Part B* **2011**, *49*, 1218 – 1233.
[21] N. Kayunkid, S. Uttiya, M. Brinkmann, *Macromolecules* **2010**, *43*, 4961 – 4967.
[22] P. Kohn, S. Huettner, H. Komber, V. Senkovskyy, R. Tkachov, A. Kiriy, R. H. Friend, U. Steiner, W. T. S. Huck, J. Sommer, M. Sommer, *J. Am. Chem. Soc.* **2012**, *134*, 4790 – 4805.
[23] M. Surin, O. Coulembier, K. Tran, J. De Winter, P. Leclère, P. Gerbaux, R. Lazzaroni, P. Dubois, *Org. Electron.* **2010**, *11*, 767 – 774.
[24] A. J. Waddon, A. Keller, D. J. Blundell, *Polymer* **1992**, *33*, 27 – 33.
[25] J. D. Roehling, I. Arslan, A. J. Moule, *J. Mater. Chem.* **2012**, *22*, 2498 – 2506.

